

# The Magnetic Properties of Sputtered $\text{Pd}_{1-x}\text{Mn}_x$ Films for Thermometry and Bolometry

R. C. Nelson,\* D. A. Sergatskov, and R. V. Duncan

Department of Physics and Astronomy, University of New Mexico, Albuquerque,  
New Mexico 87131-1520, USA

(Received December 17, 2001; revised January 24, 2002)

*The magnetic susceptibility of thin films and microstructures consisting of a  $\text{Pd}_{1-x}\text{Mn}_x$  alloy have been measured as a function of temperature and magnetic field. Sputtering from a 0.68% manganese target produced films with a concentration of approximately 0.90%, as judged by comparison with results from bulk PdMn sensitivity measurements. The thinnest films (thickness  $\leq 1.0 \mu\text{m}$ ) show significant domain scale noise below the Curie Temperature,  $T_c$ , while thicker films (thickness  $\geq 10 \mu\text{m}$ ) show reliable non-hysteretic behavior throughout the temperature range of interest. The thin films show the effects of demagnetization with the field perpendicular to the surface, but a fine screen in this orientation shows no evidence of saturation and a predictable decrease in sensitivity due to demagnetization. These films will serve as the thermometric element in a new class of bolometers and thermometers for fundamental physics applications.*

## INTRODUCTION

Bulk samples of palladium with various dilute manganese concentrations close to  $x=0.7$  atomic percent have been developed recently for paramagnetic susceptibility thermometry near 2.2 K in order to carefully study the thermophysics of the superfluid transition in pure  $^4\text{He}$ .<sup>1</sup> Similar materials with  $x \approx 0.3$  atomic percent have been developed for scientific studies near the  $^3\text{He}/^4\text{He}$  tri-critical point.<sup>2</sup> These  $\text{Pd}_{1-x}\text{Mn}_x$  materials display ideal magnetic critical behavior with Curie temperatures  $T_c(x)$  over the range of approximately 0.1 to 6 K.<sup>3</sup> Outside this range the Mn ions form a spin glass, which may result in long-term drifts and hysteretic

\* Work performed at the University of New Mexico. Present address: Department of Physics, United States Military Academy, West Point, New York 10996, USA. E-mail: raynelson@west-point.org

behavior. Even so, these materials have been successfully applied to ultra-low temperature thermometry in this glassy limit.<sup>4</sup>

Here we report on the first detailed study of the magnetic properties of thin films of these materials. These films, which display a strong temperature-dependent magnetic susceptibility comparable to their bulk value, may be used as the thermally sensitive elements in bolometers for second sound studies similar to previous experiments at Stanford,<sup>5</sup> and in steady state measurements where exceptionally high spatial and thermal resolution are required. These materials may also realize applications in radiometry, where the film is read-out through inductive coupling to a SQUID, permitting the film to be exceptionally well isolated both thermally and mechanically, with no required wire bonds to the film. Films like the ones described here may be used to make temperature measurements with a spatial resolution of about 10  $\mu\text{m}$ , and a temperature resolution of one nanokelvin at a temperature of 2.2 K. These materials may also prove useful as a replacement for semiconductor resistance thermometers that have been used traditionally in low-temperature applications.

These films are being investigated as part of a larger effort to measure the local thermal profile in the singular Kapitza resistance boundary layer,<sup>6-8</sup> and to study the nature of the onset of the normal fluid phase within this partially superfluid boundary layer.<sup>9,10</sup> Conventional high resolution thermometry is limited by thermodynamic fluctuations that scale with  $\sqrt{R}$ , where  $R$  is the thermal resistance between the thermometer and the helium.<sup>11</sup> By placing our thermometer inside the helium cell, we plan to make  $R$  so low that SQUID noise becomes the dominant factor in the total noise spectrum of the thermometer. The application being explored is the use of a PdMn screen to probe the temperature profile in the singular Kapitza resistance of a cell filled with superfluid helium with a heat flux applied. The major problems with the approach were identified as (1) achieving the desired film stoichiometry and uniformity and (2) manufacturing a hole array within the PdMn film that is sufficiently open ( $\approx 70\%$  in our case) to avoid interference with superfluid counterflow.

The film was sputtered onto a perforated substrate of fused silica. The first screen thermometer was designed with a close packed array of 182 holes, each 600  $\mu\text{m}$  in diameter and separated by walls of 125  $\mu\text{m}$ . These hole arrays were machined using an ultrasonic mill.<sup>12</sup> In this process the work piece is mounted beneath a tool head that is manufactured to the shape of the cut required. The tool head is held close to the work and vibrated at ultrasonic frequencies while a fine abrasive slurry flows between the work and the tool head. This process produces very precisely machined holes of virtually any shape in materials as hard as sapphire. While we originally sought a substrate with low thermal conductivity to minimize the

heat leak between the film (in the boundary layer) and the top of the substrate (in the bulk), and hence to maximize the thermal standoff between the bulk He II and the film, in practice the delicate substrate (which was lapped to a thickness of 125  $\mu\text{m}$  before deposition) separated from the PdMn screen on thermal cycling. Since it is easy to remove such thick films from the substrate by treatment in an ultrasonic alcohol bath, future applications will use thicker, cheaper substrates from which the film will be removed as discussed above, leaving the substrate for reuse.

## FILM DEPOSITION

If an alloy sputtering target is homogeneous, then the species with the higher sputtering rate will initially be sputtered preferentially, creating a surface layer in which the concentration of the scarcer constituent is altered by the ratio of the sputtering yields of the two materials.<sup>14,15</sup> Once the surface has equilibrated, the amount of each constituent deposited in a given time is proportional to its original density in the target and the sputtering yields are the same. Although this principle is generally valid, variation in the sputtering parameters, including ion energy and current density, as well as differences in atomic weights of the constituents can effect the final film stoichiometry.

Unfortunately, Mn is rarely deposited by sputtering, so little information is available on sputtering yields. Given this, along with the fact that Pd has one of the highest sputtering yields for any element other than the noble metals, a relatively low Mn concentration was selected to avoid a large Curie temperature,  $T_c$  and, hence, the possibility of hysteresis below the zero field  $T_c$ . Based on this decision, Target Materials Inc.,<sup>16</sup> designed a sputtering target with a nominal concentration of 0.68 atomic % Mn in the host Pd matrix. We chose this percentage because it was ten percent below the objective of 0.75 atomic % in the final film, which is the bulk concentration needed to achieve peak sensitivity at the lambda point of liquid helium.<sup>1</sup> Using this target, the Z Supporting Technologies Materials and Coatings Laboratory at Sandia National Laboratories produced three samples with a  $12.5 \pm 0.1$   $\mu\text{m}$  thick coating of PdMn alloy on Pyrex substrates 23.14 mm by 6.19 mm by 1 mm thick. After the initial testing of these samples, Sandia produced four samples with  $0.94 \pm 0.1$   $\mu\text{m}$  thick coatings on 0.5 inch round fused silica disks and coated a nominal 10  $\mu\text{m}$  of PdMn on the first two perforated screens. There is some concern that the thicker films show a tendency to delaminate after repeated thermal cycling. In applications where there must be intimate physical contact between the film and some other medium, this might be a problem. Otherwise, the film can be separated from the substrate and used independently, as discussed above.

## MEASUREMENT APPARATUS

The initial experiment used the same cryostat that Klemme *et al.* used to conduct pioneering magnetic susceptibility tests of cylindrical bulk pills of PdMn and PdFe bulk alloys in Ref. 1. The experimental setup was similar and is displayed in Fig. 1. A sample was mounted vertically into a Macor cup and potted with Tra-Bond 2151 epoxy,<sup>17</sup> then clamped in a brass ring sized to match the inside diameter of the niobium flux tube. The SQUID pickup coil of Nb-48%Ti wire was wound tightly around the sample. Regardless of the sample dimensions, each coil was wound to match the SQUID impedance of  $2.2 \mu\text{H}$ . The sample was then mounted in the center of a 6-inch long, 3/4-inch outside-diameter niobium flux-tube. The heater stage and the sample were connected with copper braid epoxied to the sample surface using Tra-Bond 2115 epoxy and screwed to the heater stage with a layer of thermally conductive grease. This resulted in excellent thermal contact and, hence, good synchronization between the measured sample temperature and the SQUID signal measuring magnetic response. The sample stage was heated and controlled with a  $1 \text{ k}\Omega$  metal-film resistor (used as a heater) and a Lake Shore Germanium Resistance Thermometer (GRT)<sup>18</sup> mounted to the bottom of the stage just below the thermal filter depicted in Fig. 1. Both GRT monitoring and temperature control were accomplished with a Linear Research LR-700 resistance bridge and

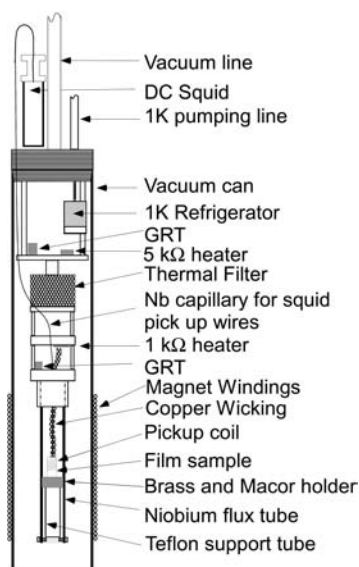


Fig. 1. Cryostat used for PdMn sensitivity measurements, as described in Ref. 1, with modifications described in this text.

controller.<sup>19</sup> This system used negative feedback to control the sample temperature at its set temperature with a precision of one microkelvin. Both the LR-700 and the Quantum Design<sup>20</sup> QD5000 DC SQUID controller were connected to the GPIB bus of a PC running the Linux operating system. A program was written to acquire the resistance of the GRT and the voltage output of the SQUID every second during a data run. A niobium wire-wound electromagnet producing 90 gauss per ampere on the centerline of the solenoid was mounted outside the vacuum can. This magnet was used to charge the Nb flux tube (see Fig. 1) during cool down, which then remained persistently superconducting to maintain a constant magnetic field on the sample film during testing. Rectangular samples with the 12.5  $\mu\text{m}$  coating, round samples with the 0.94  $\mu\text{m}$  coatings, and the 10  $\mu\text{m}$  thick screen were tested at magnetic fields ranging from 6 gauss to 250 gauss.

## DATA COLLECTION AND ANALYSIS

To collect a single data point, the experimenter would set the starting temperature, typically an excursion of 0.1 K from the previous data point, and then allow the apparatus to come to equilibrium. Then the SQUID input coil would be driven normal with a heat switch to reset any persistent currents to zero, and the data collection program would be started. After approximately two minutes the experimenter would manually change the resistance setting of the GRT by the equivalent of a 3–10 mK temperature change.

To determine the sensitivity at a particular temperature, the GRT resistance and SQUID output were plotted against one another and the equation of the best fit line through the data determined by linear regression. The slope of this line, multiplied by the instantaneous slope of the GRT resistance vs. temperature curve (based on the Chebyshev calibration polynomial supplied with the GRT by Lake Shore), and by the sensitivity setting of the SQUID controller, gives the sensitivity in units of flux quanta, ( $\phi_0$ ), per millikelvin directly. The flux quanta  $\phi_0 = h/2e = 2.07 \times 10^{-15}$  Weber. For the screen testing, the screen was mounted in a Vespel<sup>21</sup> holder designed for the Kapitza resistance boundary layer measurements. Because there was poor thermal contact between the sample and the heater stage, these measurements showed a long thermal time constant, necessitating a slightly different data analysis method. After a temperature change, the SQUID signal would asymptotically approach a final value after a period of about 40 min. The change in voltage, and hence flux, would be determined by calculating the mean of the first 100 s (before the change) and the mean of the last 100 s and taking the difference.

## RESULTS

The results of the testing of the 12.5  $\mu\text{m}$  film with the field parallel to the plane of the sample surface are presented in Fig. 2. This figure includes the results of testing for six values of the magnetic field throughout the range attainable without quenching the magnet or the flux tube.

Several features of the data are noteworthy. First, the zero field  $T_c$  is best estimated by looking at the peak of the sensitivity curve for the lowest field value tested. At 6 gauss, this gives a good estimate of  $T_c$  of 2.8 K, which would correspond to a Mn concentration in the bulk Pd of approximately 0.90 atomic %.<sup>1</sup> This is higher than the 0.68% bulk concentration in the sputtering target but still acceptable for applications around the lambda point of <sup>4</sup>He, provided that there is no evidence of hysteresis on the ferromagnetic side of the transition. A subsequent test conducted at ambient field conditions (approximately 0.3 gauss) with another of the rectangular samples showed peak sensitivity at 3.0 K. Second, the magnetic field induced shift in  $T_c$  is small, approximately 0.1 K in this film, which is much smaller than that observed in the bulk material.<sup>1</sup> Third, increasing

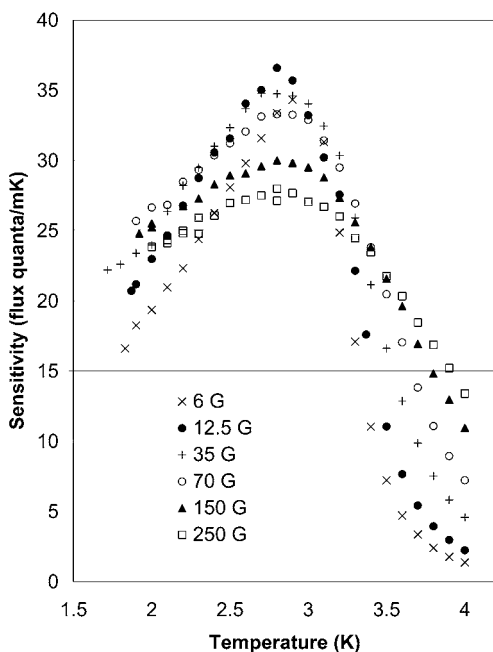


Fig. 2. Sensitivity of 12.5  $\mu\text{m}$  PdMn film at several values of magnetic field.

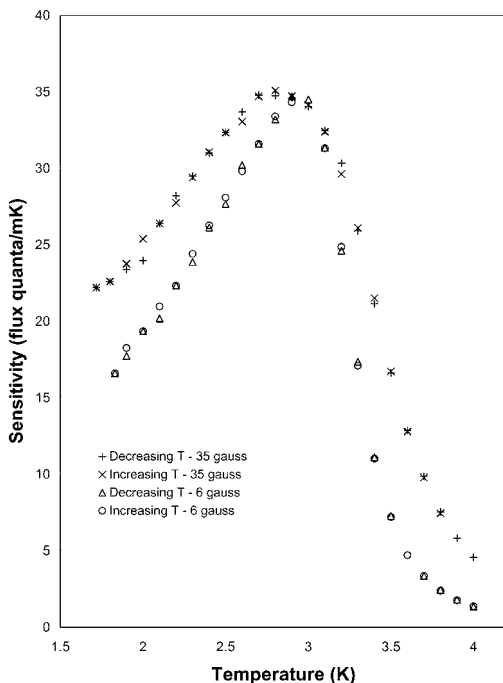


Fig. 3. Data for the 12.5  $\mu\text{m}$  film, indicating no discernible hysteresis or magnetic domain noise effects below the Curie temperature, taken at two values of the magnetic field.

the magnetic field broadens and flattens the response of the film, as can be seen from the data taken at 150 and 250 gauss. This last is evidence of magnetic saturation of the sample.

These films may be used for thermometry near  $T_\lambda$ , even if  $T_\lambda < T_c$ , provided there is no detectable hysteresis on the ferromagnetic side of the transition. Fig. 3 shows the result of a search for such hysteresis below  $T_c$ . There are two series of measurements presented, for magnetic fields of 6 and 35 gauss. In these series of measurements the temperature was decreased stepwise from 4.0 to 1.9 K, then increased stepwise back to 4.0 K. The excellent match between the data taken in each direction indicate that no hysteresis above the experimental noise level was observed. Hence a  $T_c$  above 2.2 K is no impediment to using a film of this thickness, in this orientation to the magnetic field, as a thermometer at or below the lambda point.

There was a dip in the sensitivity at several values of magnetic field at about 2.0 K in this 12.5  $\mu\text{m}$  thick film data. We took data at closer intervals around this temperature for several field values looking for evidence of

a systematic effect. There may be a feature of the data present, but higher resolution experiments with better signal to noise ratios will be necessary to explore the question further.

We tested the thinner,  $0.94 \mu\text{m}$  thick film, both with the field perpendicular to the sample and with the field parallel to the sample. The perpendicular orientation was tested to evaluate the effect of demagnetization on the sensitivity. The aspect ratio of area to thickness equals approximately 100 m in this configuration. The requirement that the normal component of the magnetic induction,  $\vec{B}$ , and the tangential component of the magnetic field,  $\vec{H}$ , be continuous across the interface between the vacuum space and the film sample lead to a spontaneous demagnetization of the sample when the ambient field is perpendicular to the sample's surface.<sup>25</sup> While the tangential components of  $\vec{H}$  are essentially zero both inside and outside the sample, the requirement that  $\vec{B}$  be continuous through the surface perpendicular to the field means that no magnetization can occur in the region close to the surface. In the geometry used previously, with the field parallel to the sample surface, the boundary condition that  $H_t$  be continuous assured that  $H_{\text{in}} = H_{\text{out}}$ . In this case,  $B_{\text{in}} = \mu H_{\text{in}}$ , and  $B$  gets

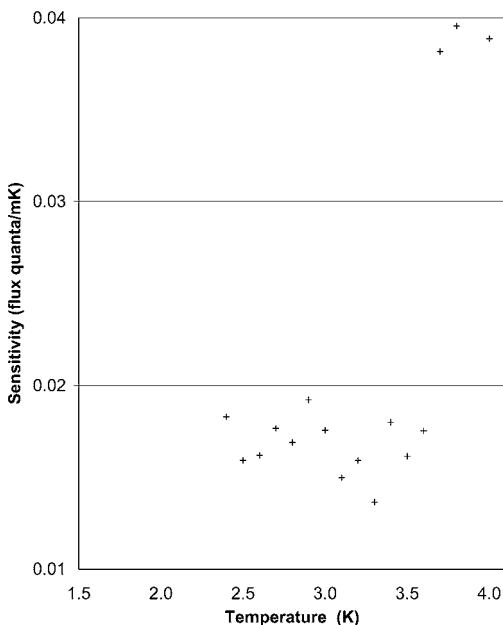


Fig. 4. Data for the  $0.94 \mu\text{m}$  film at 12.5 gauss, with the field oriented perpendicular to the sample surface, showing almost zero temperature sensitivity due to the effects of demagnetization.



large as  $\chi$ , and therefore  $\mu$ , diverges at  $T_c$ . However, in the present orientation with the field perpendicular to the sample surface, the condition in the limit of infinite aspect ratio is that the normal component of  $B$  is continuous, meaning that  $B_{\text{in}} = B_{\text{out}}$ , and therefore  $\mu = 1$  for all  $T$ . Now, since  $\mu = 1 + 4\pi\chi$ , and  $\chi(T) = \Gamma t^{-\nu}$ , as mentioned earlier, the boundary condition restriction on  $\mu$  overwhelms the expected divergence in  $\chi$ , and the sample is unable to magnetize. Unfortunately, in this orientation, with our very thin sample (thickness =  $0.94 \mu\text{m}$ ), this requirement affects most of the available magnetic material. With the sample oriented parallel to the field, this problem affects only the tiny fraction of the sample represented by the thin edges at the top and bottom of the sample. We have, in the two configurations, essentially the best and the worst possible conditions. Figure 4 displays the effect of demagnetization on the sensitivity measurements with the  $0.94 \mu\text{m}$  thick film sample with the magnetic field perpendicular to the sample surface. Figure 5 displays the results of testing of the  $0.94 \mu\text{m}$  thick film sample with the magnetic field parallel to the sample surface. This

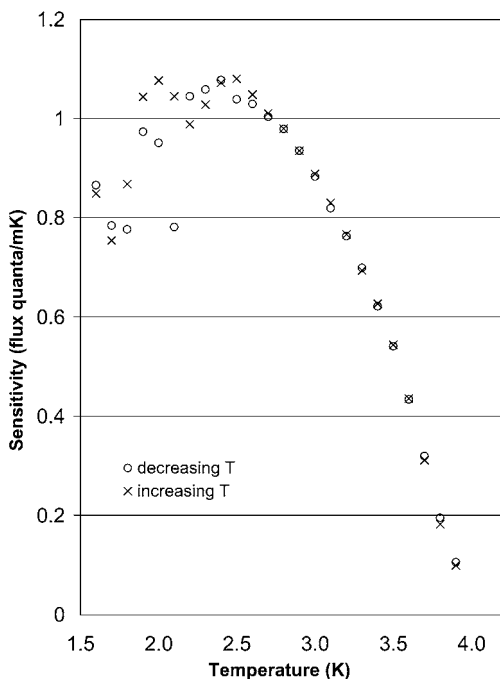


Fig. 5. Data for the  $0.94 \mu\text{m}$  film at 6 gauss, showing the emergence of magnetic noise below the ferromagnetic transition.

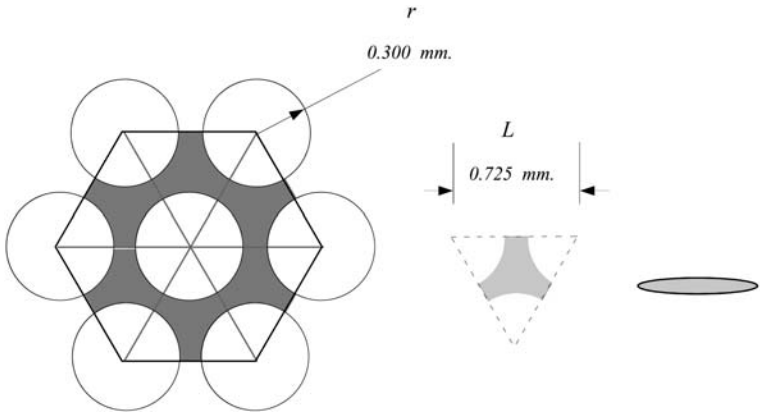


Fig. 6. Schematic representation of a unit cell in the close packed array of holes in the perforated PdMn screen thermometer. In the calculations presented here the cell volume is six times the PdMn volume depicted in the center of the figure. This cell volume is modeled as an oblate ellipsoid of revolution. The right element in this figure is a schematic cross section of this ellipsoid with the  $c$  axis vertical and the  $a$  axis horizontal. The  $b$  axis would be perpendicular to the plane of the page.

data, taken at 6 gauss, shows all of the interesting features of the data for all field values. Note (by comparing Figs. 4 and 5) that the temperature sensitivity is about 50 times larger when the thinnest film is operated with  $H$  in the plane of the film surface. For temperatures above  $T_c$ , the data is very clean and very repeatable, indicating that even such a thin film is a useful thermometer when operating in its paramagnetic state above  $T_c$ . The data below  $T_c$  show considerable noise in the sensitivity. It should be noted that the SQUID data showed an excellent signal to noise ratio, so this noise increase below  $T_c$  displayed in the data in Fig. 6 can be taken to represent a real property of the thinnest films. It is easy to speculate that the noise here is due to finite size domain effects that become quenched in thicker films. Alternatively, this increased noise may be associated with a magnetic domain structure that is incommensurate with the substrate. Regardless of the source, it is apparent that very thin films should only be used in thermometry applications above  $T_c$ . The thinner film was tested at values of magnetic field up to 70 gauss, producing similar results at every field value. One interesting feature is the shape of the data in the paramagnetic region of the graph. It is convex toward higher temperatures. The data displayed in Fig. 2 show that this shape only appears at fields above 100 gauss for the thicker film. It appears at all values of magnetic field used in the studies of the thinner film, indicating that the thin films begins to saturate at very low field values.

## SCREEN ANALYSIS AND TESTING

While the results for the thin sample oriented perpendicular to the field were not unexpected, it was hoped that the greater thickness and the greatly increased surface area parallel to the field created by perforating the screen would raise the sensitivity, thus resulting in a better material for thermometry in the configuration with the screen perpendicular to the field. Geometric factors alone, including the amount of material present, the filling fraction of the SQUID pickup loop, and the presence of the perforations would be expected to reduce the sensitivity of the screen thermometer to about 20% of that observed for the 12.5  $\mu\text{m}$  thick film sample with the magnetic field parallel to the sample surface. A simple model of the demagnetization effect in the screen yields a prediction that this sensitivity will be further reduced by a factor of 20, yielding approximately 1% of the sensitivity observed when the solid 12.5  $\mu\text{m}$  thick film was measured with H in the plane of the film, which would still provide adequate sensitivity for thermometry applications. To construct this model we first calculate the relevant dimensions of the unit cell of PdMn for the screen, represented in Fig. 6. The unit cell is six times the volume depicted in the center of the figure.

Volume of PdMn in unit cell:

$$V = 6 \left( \frac{\sqrt{3}}{4} L^2 - \frac{1}{2} \pi r^2 \right) \delta = 6A\delta \quad (1)$$

The total area parallel to the direction of the applied field, per unit cell:

$$S = \delta(3) 2\pi r = 6\delta\pi r = 6\delta D \quad (2)$$

The volume to vertical area ratio is

$$R = \frac{A\delta}{\delta D} \quad (3)$$

In these calculations,  $\delta$  is the thickness of the film. The volume to vertical area ratio of a right circular cylinder is  $r/2$ . The numerical values of these quantities are presented in Table I.

A right ellipsoidal cylinder that presents the same ratio of enclosed volume to vertical surface area as our unit cell has the minor axis equal to approximately one half the major axis. The ratios for various combinations of major and minor axes are given in Table II. To best approximate the

Table I

The Values Associated with the Above Calculations, with the Radius of the Holes in the Screen Held as a Variable

$A$	$D$	$R = A/D$
$0.965r^2$	$\pi r$	$0.31r$

volume of PdMn enclosed in a unit cell with an ellipsoid of revolution (about the smallest axis, resulting in a lozenge shape) with axes  $a$ ,  $b$ , and  $c$ , and with the major axis equal to  $r$ , we use:

$$\begin{aligned} a &= 300 \mu\text{m} \\ b &= 150 \mu\text{m} \\ c &= 5 \mu\text{m} \end{aligned} \quad (4)$$

This ellipsoid would appear as the right most element in Fig. 6. In this view the  $c$  axis is vertical in the plane of the paper. Viewed from the top of the page, the reader should imagine an ellipse with minor axis half the length of the major axis. This approximation gives an ellipsoid that is, in fact, within 10% of the actual volume of our cell. This ellipsoid has a demagnetization factor for magnetization along the  $c$  axis, given by:<sup>26</sup>

$$\frac{N}{4\pi} = 1 - \frac{cE}{a(1-e^2)^{\frac{1}{2}}} \quad (5)$$

Table II

Calculation of the Area to Circumference Ratios for Right Elliptical Cylinders of Varying Eccentricities.  $P$  Is the Circumference of an Ellipse with Major and Minor Axes  $a$  and  $b$ . The First Line Represents a Right Circular cylinder

$a$	$b$	$P$	$A$	$A/P$
1	1	6.283185	3.141593	0.5
1	0.9	5.977288	2.827433	0.473029
1	0.8	5.689666	2.513274	0.441726
1	0.7	5.42323	2.199115	0.405499
1	0.6	5.181247	1.884956	0.363803
<b>1</b>	<b>0.5</b>	<b>4.967294</b>	<b>1.570796</b>	<b>0.316228</b>
1	0.4	4.785131	1.256637	0.262613
1	0.3	4.638506	0.942478	0.203186

where  $E$  is a complete elliptic integral whose argument is  $e$ , the eccentricity of the major ellipse. The argument of this integral for our screen is 0.866 and the value of  $E$  is 1.2111.<sup>27</sup> This yields a demagnetization factor of approximately 0.96, reducing the expected sensitivity to 1% of that seen in the data of Fig. 2, as stated above.

We tested the PdMn screen in the orientation with the magnetic field perpendicular to the screen surface. The data for a wide range of magnetic field values is displayed in Fig. 7. The first and most important result is

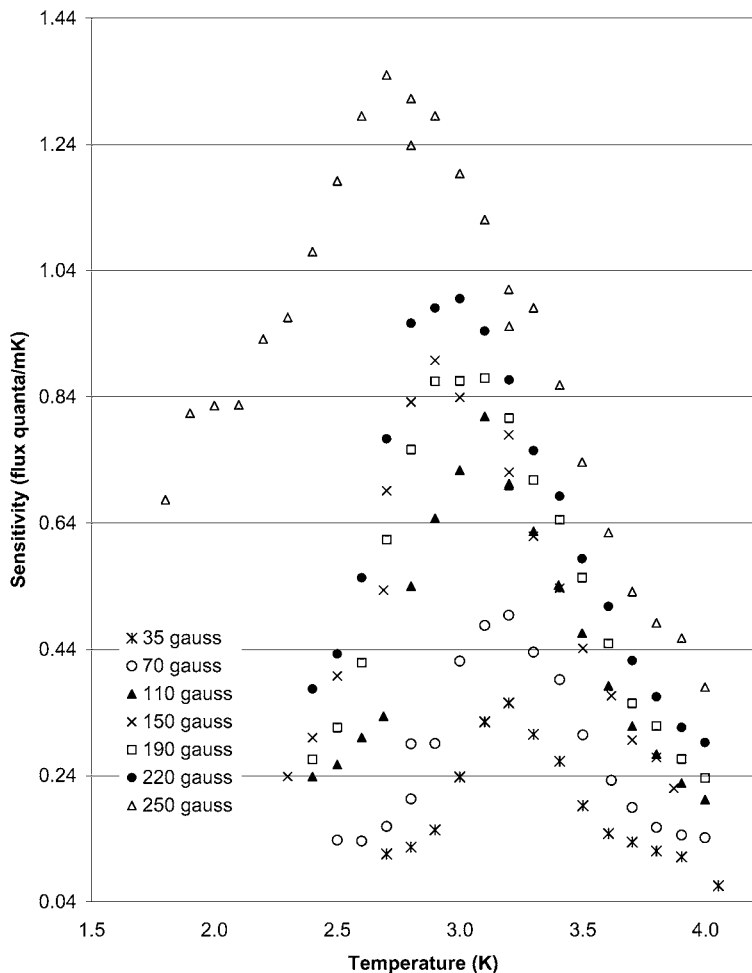


Fig. 7. Data from testing of the perforated PdMn screen for field values up to 250 gauss.

that demagnetization effects are approximately as expected from the model. Comparing the peak sensitivity of the screen at 150 G (Fig. 7) to the peak sensitivity of the bulk material at the same field (Fig. 2), the apparent ratio of the screen sensitivity with the field perpendicular to that of the solid film with the field parallel is approximately 0.8/30, which is close to the

### Sensitivity of PdMn Screen/Normalized Peak to Peak

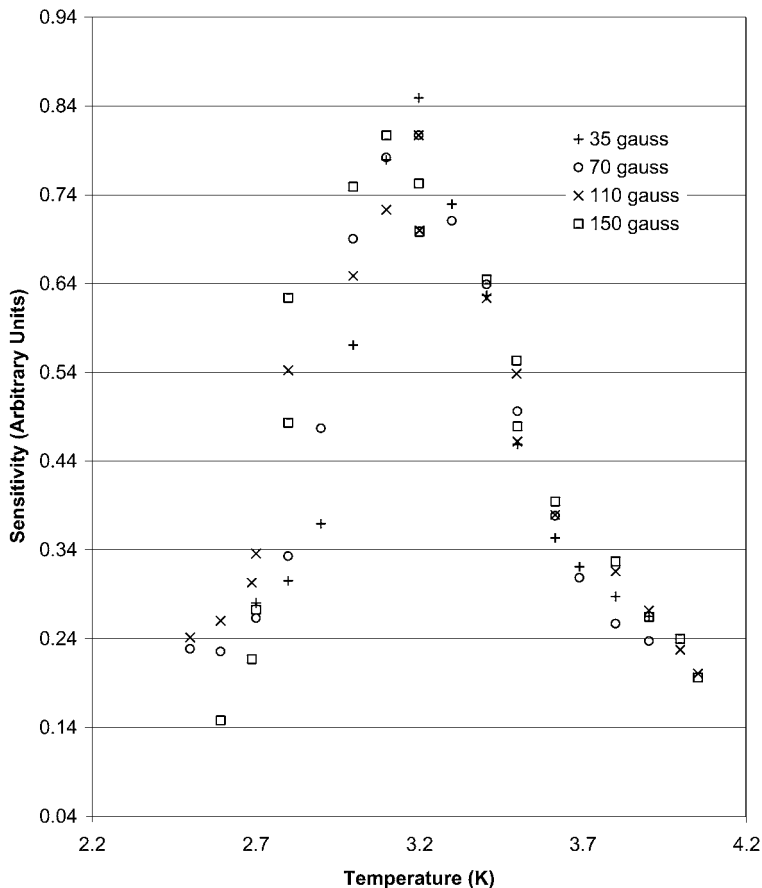


Fig. 8. Data from testing of the perforated PdMn screen, showing the results for four values of the magnetic field normalized peak to peak. The data in each set is simply scaled by the ratio of peak value of the 150 gauss data to the peak value of that set. There is no horizontal shifting of the data.

anticipated 1% discussed above. This ratio changes with field, due to an unusual scaling in the screen data. The characteristic shape of the sensitivity curve remains unchanged throughout the data. As displayed in Fig. 8, one can take any two of the sensitivity curves for the screen, from 6 gauss to 150 gauss, normalize them to the same height, and when superimposed they are essentially indistinguishable. The data show that the screen is a viable thermometer at or above its Curie temperature. Second, there is a large field induced shift in the peak sensitivity, moving the peak from 3.2 to 2.7 K over the range of field values tested. Interestingly, there is no evidence of saturation. The results of this experiment demonstrate that a fine screen of PdMn can be used as a thermometer in this orientation, but that the sputtering process must be refined to produce a  $T_c$  below 2.2 K in order to use it as a thermometer for Kapitza boundary resistance measurements.

## CONCLUSION

The sputtering process yielded an ordered film that displays the same ferromagnetic properties as the bulk samples tested by Klemme *et al.*<sup>1</sup> The practicality of a foil screen thermometer has been demonstrated in the non-ideal geometry (field perpendicular to film surface) required for the proposed Kapitza boundary resistance measurements. While these results are very encouraging, further investigations with different film stoichiometry, thicknesses, and geometries are planned to further characterize this promising material. Additionally, when our sputtering target is retired, we plan to take bulk samples from the target and determine  $T_c$  for more accurate comparison with the ordering temperature in these films.

## ACKNOWLEDGEMENTS

We wish to thank Dr. Peter Day, who first suggested the use of dilute magnetic ions in Pd for thermometry near 2 K. R. C. Nelson wishes to acknowledge the support of the United States Army. This work was performed under NASA JPL Grant No. 960494.

## REFERENCES

1. B. J. Klemme, M. J. Adriaans, P. K. Day, D. A. Sergatskov, T. L. Aselage, and R. V. Duncan, *J. Low Temp. Phys.* **116**, 147 (1999).
2. Material developed by UNM and Sandia National Laboratories, and delivered to Dr. Melora Larson, of NASA Jet Propulsion Laboratory, Principal Investigator on the EXACT experiment.
3. G. J. Nieuwenhuys, *Adv. Phys.* **24**, 515 (1975).
4. M. Jutzler, B. Schroder, K. Gloos, and F. Pobell, *Z. Phys. B* **64**, 115 (1986).
5. D. Marek, J. A. Lipa, and D. Phillips, *Phys. Rev. B* **38**, 4465 (1988).

6. R. Duncan, G. Ahlers, and V. Steinberg, *Phys. Rev. Lett.* **60**, 5 (1988).
7. M. Dingus, F. Zhong, and H. Meyer, *J. Low Temp. Phys.* **65**, 185 (1986).
8. R. Duncan and G. Ahlers, *Phys. Rev. B* **43**, 7707 (1991).
9. A. W. Harter, R. A. M. Lee, A. Chatto, X. Wu, T. C. P. Chui, and D. L. Goodstein, *Phys. Rev. Lett.* **84**, 2195 (2000).
10. R. C. Nelson, Doctoral Dissertation, University of New Mexico (2001).
11. P. Day, I. Hahn, and T. C. P. Chui, *J. Low Temp. Phys.* **107**, 359 (1997).
12. Sonic Mill, Inc., 7500 Bluewater Road NW, Albuquerque, NM, both produces the sonic mill processing equipment and has an in house fabrication shop that milled the fused silica hole arrays.
13. Y. S. Touloukian (ed.), *Thermophysical Properties of Matter*, Plenum Press, NY, (1970–1979), Vol. 2, p. 183.
14. John A. Thornton, Coating Deposition by Sputtering, in *Deposition Technologies for Films and Coatings*, Noyes Publications, Park Ridge, New Jersey (1992), pp. 170–237.
15. W. L. Patterson and G. A. Shirn, *J. Vac. Sci. Technol.* **4**, 343 (1967).
16. Target Materials, Inc., 1145 Chesapeake Avenue, Columbus, Ohio 43212.
17. Tra-Bond 2151 is a thermally conductive, electrically insulating epoxy, a product of TRACON, Inc., 45 Wiggins Avenue, Bedford, MA 01730. Tra-Bond 2115 is a lower viscosity, non silica based epoxy made by the same company.
18. The germanium resistance thermometer used was a Lake Shore Model GR-200A-1500, Lake Shore Cryotronics, Inc., 64 East Walnut St., Westerville, OH 43081.
19. Linear Research, Inc., 5231 Cushman Place, Suite 21, San Diego, CA, 92110.
20. Quantum Design, Inc., 11578 Sorrento Valley Road San Diego, CA, 92121.
21. Vespel polyimide is a trademark of Dupont.
22. H. Eugene Stanley, *Introduction to Phase Transitions and Critical Phenomena*, Oxford University Press, New York (1971).
23. J. J. Binney, N. J. Dowrick, A. J. Fisher, and M. E. J. Newman, *The Theory of Critical Phenomena*, Oxford University Press, New York (1992).
24. G. Ahlers, in *The Physics of Liquid and Solid Helium*, K. H. Bennemann and J. B. Ketterson (eds.), Wiley, New York (1976–78), Vol. 1, Ch. 2.
25. See for example, J. D. Jackson, *Classical Electrodynamics*, John Wiley (1975), pp. 187–191.
26. J. A. Osborn, *Phys. Rev.* **67**, 351 (1945)
27. W. H. Beyer (ed.), *Standard Mathematical Tables, 25th Ed.*, CRC Press (1978), p. 435.